

Thermodynamic aspects of the glass transition phenomenon. II. Molecular liquids with variable interactions

C. Alba-Simionesco, J. Fan, and C. A. Angell

Citation: *J. Chem. Phys.* **110**, 5262 (1999); doi: 10.1063/1.478800

View online: <http://dx.doi.org/10.1063/1.478800>

View Table of Contents: <http://jcp.aip.org/resource/1/JCPSA6/v110/i11>

Published by the AIP Publishing LLC.

Additional information on J. Chem. Phys.

Journal Homepage: <http://jcp.aip.org/>

Journal Information: http://jcp.aip.org/about/about_the_journal

Top downloads: http://jcp.aip.org/features/most_downloaded

Information for Authors: <http://jcp.aip.org/authors>

ADVERTISEMENT



Explore the **Most Cited**
Collection in Applied Physics

AIP
Publishing

Thermodynamic aspects of the glass transition phenomenon. II. molecular liquids with variable interactions

C. Alba-Simionesco

Université Paris-Sud, Laboratoire de Chimie Physique des Matériaux Amorphes Unité Associée au C.N.R.S. no. 1104, Orsay, France

J. Fan and C. A. Angell^{a)}

Department of Chemistry, Arizona State University, Tempe, Arizona 85287

(Received 29 December 1997; accepted 24 November 1998)

As a contribution to the understanding of the thermodynamics of the glass transition phenomenon a series of molecules having the same steric character, but differing in the strength and nature of intermolecular interactions, has been investigated. The series is based on systematic changes of substituents on disubstituted benzene ring compounds, the simplest example of which is meta-xylene. Meta-isomers are chosen in each instance because of their greater tendency to supercool. In particular, *m*-fluoroaniline cannot be crystallized at ambient pressure. The principal measurements performed were of heat capacity and enthalpy change, using the technique of differential scanning calorimetry, and these have been examined in the light of literature data on the liquid viscosities and some recent data for dielectric relaxation. As the strength of hydrogen-bonding interactions between the ring substituents on adjacent molecules increases, the glass transition temperature T_g increases by almost 100 degrees from the lowest value in the series, 122.5 K, for *m*-fluorotoluene. Empirical rules involving T_b/T_m and T_g/T_m are found wanting. The important thermodynamic characteristic of the glass transition, viz., the change in heat capacity at the glass transition, ΔC_p , remains approximately constant until the $-\text{OH}$ substituent is introduced, whereupon a new element appears. This is a specific component of ΔC_p which appears at temperatures above an initially small jump at T_g . It is well accounted for by the addition of a two-state H-bond breaking component (with the usual $\text{H}\cdots\text{OH}$ bond energy) to the total excess heat capacity. The liquid ground state (or Kauzmann) temperature T_K assessed from thermodynamic data acquired in this study, falls 20%–30% below the glass transition temperature. From the limited transport data available, these liquids appear to be quite fragile in character implying that the phenyl group influence dominates the hydrogen bond factor which has often seemed responsible for decreased fragility. In the case of cresol the hydrogen bonding apparently produces dielectric/shear relaxation anomalies of a character previously only seen in certain aliphatic monoalcohols.

© 1999 American Institute of Physics. [S0021-9606(99)50909-4]

I. INTRODUCTION

In the past few years the glass transition phenomenon has won general recognition as one of the outstanding unsolved problems in condensed matter physics. There are currently a variety of approaches being taken to interpret the rather rich phenomenology presented by the many different types of liquid which can be observed to vitrify during cooling (or compression). These are distinguished by their different emphases on solid state^{1–3} vs liquid state^{4–8} processes and their concern^{4,5,8} or otherwise^{6,7} with a thermodynamic underpinning of the phenomenon. Reviews of different aspects of the field by several authors were given in a recent special issue of *Science*.⁹

Much attention has been given recently to purely dynamic approaches, based on mode-coupling theory (MCT).^{6,7} In these it is recognized that the glass transition, and the attendant loss of ergodicity, has thermodynamic conse-

quences (viz. breaks in heat capacity, C_p and compressibility κ_T) which are calculable.⁷ However, these are seen as incidental to, rather than an essential part of, the phenomenon. By contrast, there are other approaches^{4,5,8} which, while also taking the liquid state as starting point and recognizing the essentially kinetic character of the laboratory time scale glass transition phenomenon, interpret it as the kinetic consequence of either (i) an evolving *thermodynamic* state,^{4,5} or (ii) a narrowly avoided thermodynamic event associated with frustrated clustering.⁸ Implicit in the first of these latter approaches^{4,5} is the recognition that the evolution would give rise, at equilibrium, to a phase transition,^{4,5,10} or at least to a strong C_p anomaly,² on time scales much longer than those customary in laboratory studies.

The mode coupling approach, and the low temperature phase transition approach, are not mutually exclusive but may be viewed as descriptive of different stages of the cool-down process. The first stage described by MCT concerns the behavior in the free liquid state as the system falls with decreasing temperature into one of the higher energy minima

^{a)}This work was initiated while the authors Alba-Simionesco and Angell were at Purdue University. Electronic mail: caa@asu.edu

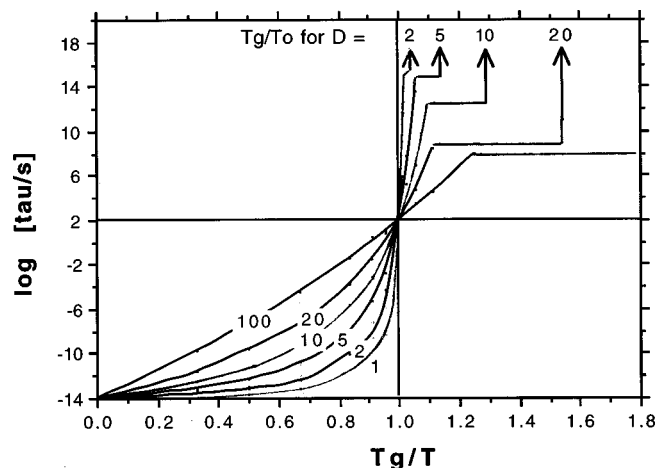


FIG. 1. Variations of the relaxation time with temperature for liquids of differing fragility characterized by the parameter D according to the (modified) Vogel–Fulcher equation, Eq. (3). The plots show the initial parts of the curves below T_g , and an indication of the temperatures T_g/T_0 at which the relaxation times would diverge, for each value of D .

on the Goldstein–Stillinger energy landscape¹¹ whereupon the mechanism of relaxation changes to one of cooperative exploration of the landscape, and the relaxation time temperature dependence comes under the control of the configurational entropy S_c , in the manner suggested by Adam and Gibbs⁴

$$\tau = \tau_0 \exp C\Delta\mu/TS_c. \quad (1)$$

Here $\Delta\mu$ is a free energy barrier per particle opposing the cooperative molecular rearrangement, C is a constant, and S_c is the entropy generated as temperature T rises above the ground state (Kauzmann) temperature T_K according to

$$S_c = \int_{T_K}^T \frac{\Delta C_p}{T} dT. \quad (2)$$

Here ΔC_p is usually taken as the difference in heat capacity between liquid and crystal states though this should usually overestimate the strictly configurational component of the total excess entropy.¹² If ΔC_p varies hyperbolically with T , ($\Delta C_p = K/T$), as is the simplest description of the observations, Eqs. (2) and (1) together yield the Vogel–Fulcher–Tammann (VFT) equation for the relaxation time in the form

$$\begin{aligned} \tau/s &= \tau_0 \exp C\Delta\mu T_K/K(T - T_K) \\ &= \tau_0 \exp DT_K/(T - T_K), \end{aligned} \quad (3)$$

with B of the VFT equation $= DT_K$, and T_0 identified with the Kauzmann temperature T_K (concerning which more will be said below). The parameter D (the liquid “strength” parameter, characterizes the departure from Arrhenius behavior, which is small if D is large.

In Fig. 1, Eq. (3), with τ_0 fixed at 10^{-14} s, is plotted for various D values. The set of curves qualitatively reproduces the so-called “strong–fragile” pattern of behavior found for relaxation times of viscous liquids.¹³ However, Fig. 1 also shows part of the behavior expected at $T_g/T > 1$ which usually cannot be presented in experimental plots because the time scales become too long for ergodic state measurements.

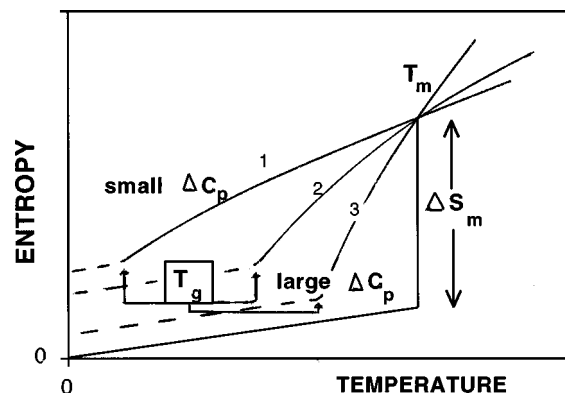


FIG. 2. Plots showing the variation of the excess entropy with temperature below T_g for strong and fragile liquids, using reduced co-ordinates, to highlight the Kauzmann vanishing entropy crisis for fragile liquids.

The figure shows how the temperatures T_g/T_0 , at which relaxation time diverges, varies with the parameter D according to Eq. (3). The relation is a linear one.

Equation (3) shows that the departure from Arrhenius behavior indicated by the value of D in Fig. 1 can be determined either by the thermodynamic (density of configurational states) parameter $K = T_K \Delta C_p(T_K)$, or by the kinetic (cooperative energy barrier) term $\Delta\mu$. It is possible for a liquid to be thermodynamically fragile (large K) but behave in an intermediate fashion due to large barriers between configurational states. Cases in question could be hydrogen-bonded systems like the alcohols which have D values of 12 or higher despite large values of ΔC_p .¹³ The different possibilities have been illustrated graphically by “landscape” diagrams, in Refs. 13(b) and 14.

A further and challenging example of this distinction is found in the contrast of the two 7-carbon liquids methyl cyclohexane and toluene. Toluene, which was the subject of a previous paper in this series,¹⁵ is fragile in character while methyl cyclohexane, which differs only by six protons (and the consequent absence of a planar structure), behaves in a rather different way, intermediate between strong and fragile extremes.

An additional distinction of importance between such liquids is that the fragile toluene at its T_g is much closer to the thermodynamic limit on liquid state behavior, the Kauzmann temperature T_K , than is methyl cyclohexane. The Kauzmann limit¹⁶ is defined by the intersection of the supercooled liquid entropy curve (when extrapolated below the kinetically determined T_g) and the crystal entropy curve, as illustrated by the alternative thermodynamic paths for cooling from the liquid state above the melting point illustrated in Fig. 2. For a wide variety of liquids,¹⁷ T_K evaluated in this manner is found experimentally to be within a few percent of the value found from fitting relaxation time data to Eq. (3) provided τ_0 from the fit has the physical value of about 10^{-14} s (corresponding to a short wavelength quasi-lattice vibration time). It would seem that at or before T_K some very significant changes in the internally equilibrated liquid state heat capacity must occur in order to avoid the generation of an amorphous state with lower total entropy than that of the crystal. The possibility of observing at least the early stages

TABLE I. Physical properties of di-substituted benzenes.

Substance	Substituents	T_b (K)	T_m (K)	T_b/T_m	T_g (K)	T_b/T_g	T_g/T_m	μ Debye	ϵ_0 (°C)
o-fluorotoluene		388	211	1.84				1.37 (g)	4.22 (30 °C)
m-fluorotoluene	–F, –CH ₃	387	185	2.09	122.5	3.16	0.66	1.86 (g)	5.42 (30 °C)
p-fluorotoluene		385	215	1.79				2.00 (g)	5.86 (30 °C)
o-xylene		417	248	1.68					2.568 (20)
m-xylene	–CH ₃ , –CH ₃	412.1	225.3	1.83	(125.5) ^a	3.28	0.56	0.34	2.374 (20)
p-xylene		411.1	286.4	1.44				0	2.270 (20)
o-fluoroaniline		467.8	238.6	1.96	174		0.73		
m-fluoroaniline	–F, –NH ₂	459	~220 [#]	...	173	2.65	0.79 [#]	2.4	
p-fluoroaniline		460	271.2	1.70					
o-toluidine		473.43	249.5	1.90				1.60 (25)	6.34 (18 °C)
m-toluidine	–CH ₃ , –NH ₂	476.4	242.8	1.96	187	2.55	0.77	1.45 (25)	5.95 (18 °C)
p-toluidine		473.75	316.9	1.50				1.52 (25)	4.98 (54 °C)
o-fluorophenol		445.2	289.3	1.54					
m-fluorophenol	–F, –OH	451	286	1.57	191	2.36	0.67		
p-fluorophenol		458.2	320.2	1.43					
o-cresol		464.15	304.14	1.53				1.45 (25)	11.5 (25 °C)
m-cresol	–CH ₃ , –OH	475.4	285	1.67	198	2.40	0.69	1.61 (20.3)	11.8 (25 °C)
p-cresol		475.1	308	1.54				1.54	9.9 (58 °C)
m-toluidine + fluorobenz. acid	CH ₃ , NH ₂ F, COOH		337		227		0.67		
		...							

^aExtrapolated from binary solution data.

of the equilibrium phenomenon, which would be of considerable theoretical interest, should be greater the more “fragile” the liquid. The theoretical denial of the possibility of a true singularity in supercooled liquids at low temperatures¹⁸ can only increase the likelihood that the onset of an equilibrium C_p anomaly will eventually be observable. There are, accordingly, good reasons for a systematic study of the thermodynamic behavior of liquids of related structure near and below their glass transition temperatures.

In the previous paper¹⁵ we examined the conditions under which xylene could be vitrified, and compared the properties of the supercooled states of toluene and xylene with those of their paraffinic analogs. In this paper we have chosen to characterize calorimetrically the xylenes and a series of related molecular liquids which have similar meta-disubstituted benzene structures but differ in dipole moments and intermolecular hydrogen bond strengths. In the series chosen for study—m-fluorotoluene mFT, m-xylene mXL, m-fluoroaniline mFA, m-toluidine mTD, m-fluorophenol mFP, and m-cresol mCS—the glass transition temperature almost doubles (122→199 K). An additional case of still higher T_g , 227 K, has been obtained by mixing m-toluidine with m-fluorobenzoic acid, and even higher values may be obtained with the more strongly H-bonding dihydroxy benzenes.¹⁹ A number of studies on individual examples of these disubstituted benzenes have been reported²⁰ since this initial study was made. Here we provide the thermodynamic characterization and analysis which is needed as a basis for the more detailed studies.

II. EXPERIMENT

A. Materials

Since this was intended as a survey study of changes of entropy and heat capacity at the fusion point and of heat

capacity at the glass transition temperature, and since none of these are sensitive within our experimental precision to small changes of composition, the liquids studied, while of the highest purity available commercially, were used without further purification. The stated purity levels were mFT (Eastman >99%), mFA (Aldrich >99%), mTD (>99%, pTD, 0.5%), mFP (Aldrich 98%, Fluka >98%), mCS (Aldrich >99%).

B. Heat capacity measurements

Heat capacities of liquid and glassy states, and of crystalline states in all cases except fluoroaniline (which could not be induced to crystallize), were determined over the temperature range 100–273 K by differential scanning calorimetry, using the Perkin Elmer DSC-4 instrument for an initial survey, and a Setaram model 121 for more quantitative measurements. The latter instrument has a more limited low temperature range, >–100 °C, than the DSC-4 but has a considerably more stable baseline. It was found possible repeatedly to reproduce the known heat capacity of o-terphenyl to within 3% over the temperature range 250–350 K with the Setaram instrument. Thus the data reported for m-xylene and m-fluorotoluene are to be considered less reliable than the remainder (though the values reported for toluene in our initial study¹⁵ have recently been verified within 3% by the definitive work of Yamamuro *et al.*²¹). For each substance a number between two and seven separate scans were made, using scan rates of 10 K/min in the Perkin–Elmer (PE) DSC-4 studies, and 10, 5, and 2 K/min (mostly 10 K/min) in the Setaram 121 studies. The lower scan rates could only be used for samples with high T_g values, e.g., mCS, mTD. Heats of fusion were measured to $\pm 1.0\%$ by reference to a standard indium sample using 2 K/min scan rates.

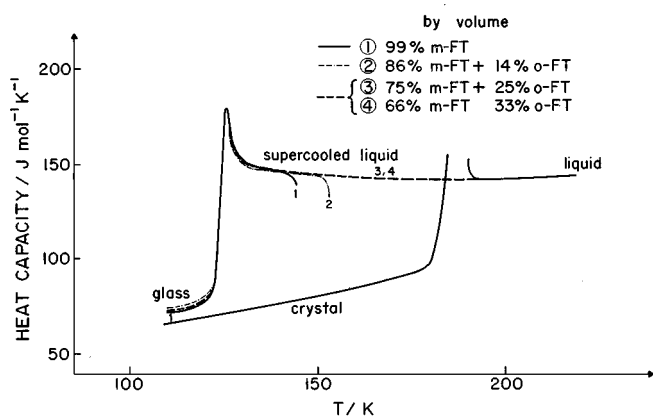


FIG. 3. Heat capacity of m-fluorotoluene crystal and liquid, including liquid mixtures with different mole fractions of o-fluorotoluene, as indicated in legend.

Samples of mass 25–30 mg were contained in hermetically sealed aluminum pans for the PE DSC studies and in resealable stainless steel capsules for the Setaram DSC studies, and weighed before and after measurement to verify integrity of samples studied.

III. RESULTS

Glass transition temperatures found for the liquids of this study are collected in Table I together with other data which will be used in the Discussion section. The liquids all crystallized during heating scans except for m-fluoroaniline (which in this work resisted all attempts to crystallize it, though it can be crystallized under pressure²⁰), and m-toluidine [which in this study only crystallized if it had first been cooled below its β -glass transition temperature, 55 K below T_g (see discussion and Ref. 22)]. Thus for most cases the supercooled liquid heat capacity data are incomplete.

One way of eliminating the latter data gap is to repeat the study using mixtures of ortho- and meta isomers. This is illustrated in Fig. 3 for the case of the fluorotoluenes, which yielded one of the most consistent sets of data of the DSC-4 study and for which the T_g is out of range of the Setaram instrument. Figure 3 shows data for the pure MFT, and for some mixtures with the o-isomer. It is seen that the heat capacity of liquid fluorotoluene is insensitive to the isomer mixture within our experimental accuracy.

For other liquids, isomer mixtures were not used. Dashed lines on the plots show the most plausible connections of the heat capacity of the stable liquid to that of the supercooled liquid before crystallization. With the Setaram instrument, some measurements were also made during steady cooling to reduce the data gap. The temperature calibration for measurements made during cooling can be made using liquid crystal mesophase transitions e.g., the nematic–isotropic transition, as standards, since the high temperature phases do not supercool.²³

Note, in Fig. 3, the ~ 10 J/mol K gap between glass and crystal heat capacity data at T_g . This is similar to our earlier study of toluene¹⁵ and, with greater accuracy, in the adiabatic calorimetry studies of toluene²¹ and isopropyl benzene.²⁴ This excess heat capacity in the glass is associated with fast local rearrangement processes (the β -relaxation) which are not frozen out when long range diffusion ceases. They freeze out at a much lower temperature in a subsidiary weak relaxational “transition.” First observed by Kishimoto *et al.*²⁴ for isopropylbenzene at $0.75T_g$, this “ β glass transition” has also been observed by us in the case of m-toluidine (see below) and has recently been carefully characterized for several molecular liquids by Oguni and co-workers.²² The β glass transition seems to have a special significance in the case of m-toluidine.

Data for m-toluidine, for experimental cycles involving cooling to just above, and just below, the β glass transition,

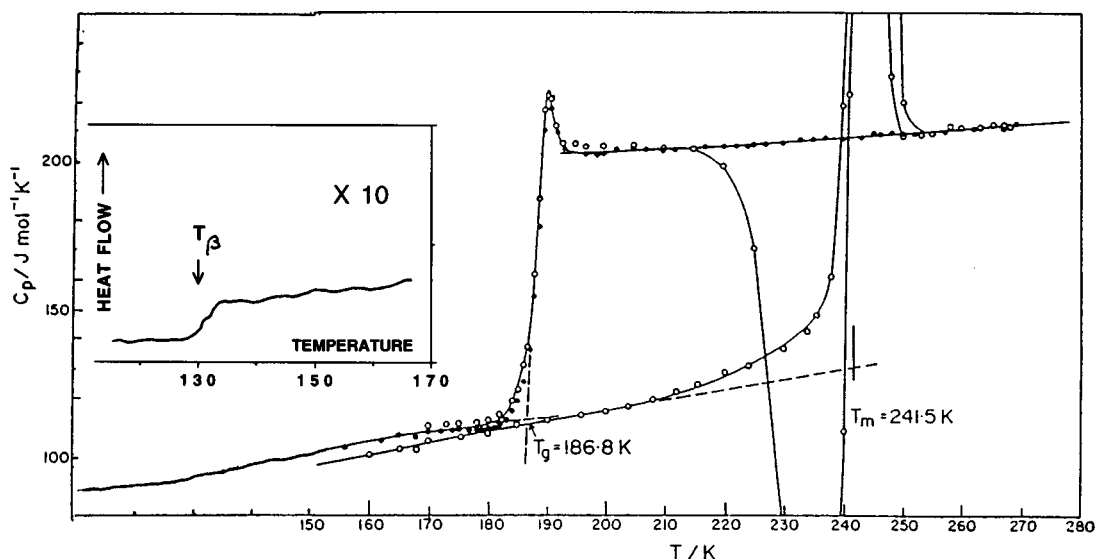


FIG. 4. Heat capacity vs temperature for liquid, glass, and crystal states of m-toluidine according to the present DSC-4 measurements. Insert shows the heat flow behavior near the β -glass transition temperature at 128 K on magnified (10 times) scale. Some data obtained with the Setaram Model 111 calorimeter, which are about 10% lower in value, but lack the low temperature data, are shown in Fig. 5. Inset: β -glass transition at 13 K, at high sensitivity. Repeat scans did not show as sharp a jump, but the transition was always evident.

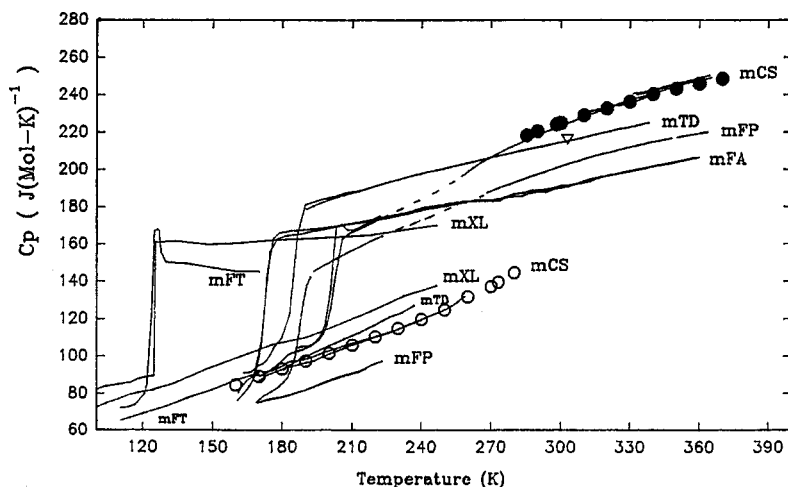


FIG. 5. Collection of data for all the *m*-disubstituted benzenes of this study showing crossovers in values at higher temperatures in the cases of hydroxylic H-bonded cases. Data from Setaram instrument are presented in place of DSC-7 data when both are available, and literature data are included where available [mCS, liquid above T_m and crystal (Ref. 58), and mTD, datum at room temperature (Ref. 60)].

are shown in Fig. 4. The β glass transition is shown in the insert at a magnification of ~ 10 times relative to the primary relaxation. The curves in Fig. 4 illustrate the interesting and so-far-unexplained fact that if liquid *m*-toluidine in our small DSC samples is cooled down to, but not below, its β "glass" transition temperature, it will not crystallize on reheating. However, in this study, if it was cooled below this point the liquid crystallized during warm-up at the (reproducible) temperature shown in Fig. 4. (This behavior is not reproduced with larger samples.²⁰)

Heat capacity vs temperature relations for other liquids of the study, mFA, mFP, and mCS are shown in Fig. 5 together with the data for the other systems in the series. The figure contains also the crystal state data and literature data where available (Fig. 5 caption) as well. When twin lines appear, they represent repeat scans at different scan rates with the Setaram 121 and serve as an index of reproducibility. Single lines for low T_g samples represent an average of mul-

tiple runs. The differences in the behavior observed in the liquid state of mFA, mTD, and mCS are particularly pronounced, but there are also marked differences in the glassy and crystalline state behavior. A summary of observations from the calorimetric studies is contained in Table II along with derived quantities to be discussed below.

IV. DISCUSSION

A. Glass formation: The T_b/T_m and T_g/T_m rules

We consider first some questions about glass formation and empirical rules raised by this work. Among molecular liquids a well-known and useful guideline to glass-forming ability has been the so-called $T_b/T_m \geq 2$ rule. The rule asserts that molecular liquids fail to crystallize on cooling at reasonably fast rates (e.g., $Q = dT/dT \geq -100$ K/min) if the boiling point exceeds the melting point by a factor of 2 or more. Complementary explanations of this rule have been

TABLE II. Calorimetric properties of glassforming disubstituted benzenes.^a

Substance (instrument)	T_g	$C_p(g)$ at T_g	$C_p(l)$ at T_g	ΔC_p at T_g	ΔS_f J/mol/K	T_K [Eq. (9)]	T_g/T_K [Eq. (9)]	S_{ex} (at T_g) J/mol [Eq. (8)]
<i>m</i> -fluorotol(PE) (DSC-4)	122.5	70, 77	149	74	48.7	98.8 (97.1)	1.24 (1.26)	18.3 (18)
<i>m</i> -xylene (PE DCS-4)	125.5 (extrap)	72	144	72	51.3	96.3 (98.5)	<1.30 (1.29)	19.5
<i>m</i> -fluoroaniline (PE 4)	173	74.8	161	86	no	no		
(Setaram 111)	173	86.7	164.4	77.7	crystal	crystal,		
DSC-2 (Ref. 42)	169	89.1	170	80.9	hence	hence		
.....adiabatic cal (Ref. 56)					no ΔS_f	no T_K		
<i>m</i> -toluidine (PE DSC-4)	187	110	202	90		160	1.17	14.8
(Setaram 111)	182, 183	100	182	82	37.7	151 (153)	1.20, 1.21 (1.19)	15.5 (13.2)
(PE DSC 7)					36.9			
.....adiabatic cal (Ref. 56)					37.0			
<i>m</i> -fluorophenol (PE 4)	191	98		(76.5)	(35.3)	~(142)	~(1.34)	(5.32)
(Setaram 111)	189.4	88	143.2	54.4	42.5	145	1.31	14.7
<i>m</i> -cresol (PE DSC-4)	198.6	83	152.5	67.5		168	1.18	
(Setaram 111)	198.5	108	162	54	37.1	159	1.25	13.5
<i>m</i> -toluidine + fluorobenzoic acid (PE)	227	212	318	25.9?				

^aValues in parentheses are calculated from minimal data using Eq. (9).

given by Turnbull and Cohen,²⁵ and by Angell, *et al.*²⁶ The rule applies well to the fluorotoluene family in which m-fluorotoluene, the only isomer which is glass-forming at ordinary quenching rates ($>100 \text{ K min}^{-1}$) is also the only isomer for which T_b/T_m exceeds two, see Table I. It also predicts the lack of glass-forming ability amongst the pure xylenes, and accounts for the fact that a eutectic mixture of isomers, for which the eutectic temperature T_E is the effective melting point, can be more easily vitrified, $T_b/T_E = 1.98$ (though why an off-eutectic mixture as used in the present work should be even more resistant to crystallization than the eutectic itself, requires a more specific explanation).

On the other hand, the T_b/T_m rule totally fails to predict the occurrence of easy vitrification in the case of the higher melting members of the present series, m-fluorophenol and m-cresol, each of which have T_b/T_m less than 1.7. Small values of T_b/T_m for glassforming H-bonded liquids have been noted previously,²⁶ but the explanation provided (in terms of low fragility) would not seem to apply to the present cases.

Interestingly enough, both of these substances violating the T_b/T_m rule conform satisfactorily to a further empirical rule which connects the glass transition temperature to the melting point, viz. the $T_g/T_m \approx \frac{2}{3}$ rule.²⁷ With respect to this latter rule, it is the middle members of the series (fluoroaniline and toluidine) which now appear exceptional, with T_g much closer to T_m than usual. mFA is particularly interesting since even the o-isomer (which is glass forming but can be crystallized) has a T_g almost $\frac{3}{4}$ of T_m . In the present work, mFA could not be crystallized implying T_g even closer to T_m . mFA has subsequently been crystallized under high pressure,²⁰ and an approximate normal pressure melting point has been estimated. It corresponds closely with the value estimated in Table I from the family relations between o-, m-, and p-isomer melting points in the other compounds.

The conclusions of this section are,

(i) T_b/T_m anomalies exist but their explanation must await a detailed study of viscosity, and of the nucleation and growth kinetics, and perhaps also of anomalous boiling characteristics for these systems.

(ii) Exceptions to “the $\frac{2}{3}$ rule” exist, but this is because the $\frac{2}{3}$ rule connecting T_g to T_m is not a rule so much as a tautology. The “rule” exists because substances which do not obey the rule normally do not get recorded: Substances with low T_g/T_m do not vitrify under normal cooling conditions so T_g is not recorded, and substances with high values (like mFA) do not crystallize so T_m is not recorded. When efforts are made to broaden the range of data by including fast quenched and pressure-crystallized substances, the $\frac{2}{3}$ rule no longer holds.

B. The glass transition temperatures

The order observed for the glass transition temperatures is believed to reflect a combination of van der Waals and hydrogen bonding interaction effects. For instance it is the weaker van der Waals interactions between F atoms, and the tendency of fluorine to withdraw electron density from the benzene ring, which is presumably responsible for the for m-fluorotoluene having a lower T_g than m-xylene, despite

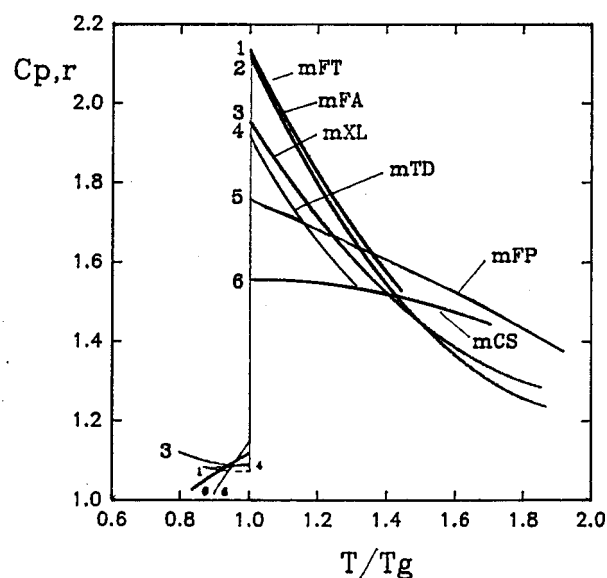


FIG. 6. Relative values of liquid heat capacity obtained by ratioing liquid to crystal values (glass in case of the noncrystallizing mFA), displayed on a T_g -reduced temperature scale. Note large (>2.0) $C_{p,r}$ values for mTD and mFA.

the presence of much larger dipole–dipole interactions in the former case. The relative unimportance of the dipole–dipole interactions in determining T_g is further attested to by the data for mFA and mTD collected in Table I.

Comparison of the dipole moments with static dielectric constants, however, suggests that considerable orientational ordering effects are present in m-cresol and to a lesser extent in m-fluorophenol as might be expected from the tendency of $-\text{OH}$ groups to hydrogen bond to one another. The H-bonding is presumably also the factor most involved in fixing the relation of the boiling points. Since the order of boiling points is also the order of glass transitions we may conclude that the difference in T_g values originates mainly in differences in the strength of intermolecular H-bonding. This conclusion is supported by the further increase in T_g found in the 1:1 m-toluidine+fluorobenzoic acid mixture in which strong hydrogen bonding between the basic $-\text{NH}_2$ group and the carboxylic acid groups must occur.

C. The heat capacity jump at T_g and the liquid excess heat capacity

The change in heat capacity at T_g , ΔC_p —defined here as the excess of liquid over glass extrapolated to T_g from shortly above (liquid) and shortly below (glass)—shows surprising variations through the series. While similar for the early members, fluorotoluene and xylene, it increases strongly for fluoroaniline and toluidene, and then plunges to much lower values for fluorophenol and cresol. At the same time the shape of the excess heat capacity of liquid over crystal (or over glass for the uncrystallizable fluoroaniline) changes considerably, as shown in Fig. 6. It appears that in the latter members of the series a component of the excess heat capacity has become detached from that contributing the normal increase at T_g and moved up to higher temperatures.

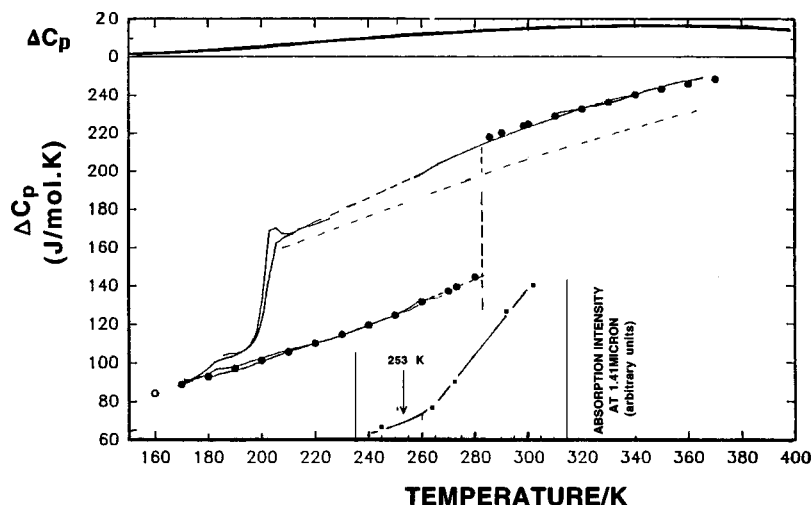


FIG. 7. Heat capacities of liquid, glass, and crystalline states of *o*-cresol. Dashed line shows residual liquid heat capacity after subtraction of the component assigned to the breaking of H-bonds. The latter is calculated using Eqs. (6) and (7) with parameters $\Delta H = 10.5$ kJ/mol, $\Delta S = 19$ J/mol K. This calculated component is shown in the upper section of the diagram as a solid line. The subtraction resolves the anomalous appearance of the heat capacity for this liquid.

The case of *m*-cresol mCS is the most clear cut and in Fig. 7 we separate out from Fig. 5 the data for this case for special consideration.

We believe this separate component of the heat capacity, indicated by the excess of C_p above the dashed line in Fig. 7, is to be associated with a distinct and separate contribution to the total excess heat capacity due to the breaking of hydrogen bonds between the $-\text{OH}$ groups on separate molecules, and support this assignment with some overtone infrared (IR) spectra to be reported separately.²⁸ The essential component of this spectral study is shown in the insert to Fig. 7. The insert shows how, during cooling, a spectral component associated with ruptured hydrogen bonds (the “free $-\text{OH}$ ” band)^{29,30} decreases (in favor of a component associated with intact bonds). In the case of *m*-cresol, this component almost vanishes before T_g is reached, while in fluorophenol some H-bonds still remain broken when the glass transition is reached and then are frozen in—as in the case of glycerol.³¹ The structure of crystalline cresol³² reveals the presence of trimeric units hydrogen bonded together via a central triangle of the three $-\text{OH}$ groups, and it is probably the entropically favored break-up of such units above T_g which provides the source of the add-on heat capacity component.

We can quantify this contribution and locate it correctly in temperature (relative to the T_g), using the equations for a “bond on-bond off” model³³ with reasonable values assigned to the enthalpy and entropy of bond rupture. The relations are those for a simple Schottky two level system modified to include an excitation entropy ΔS

$$\text{“on”} \leftrightarrow \text{“off”} = A \leftrightarrow B$$

$$K = [A]/[B] = X_B/(1 - X_B), \quad (4)$$

$$\Delta G = \Delta H - T\Delta S = RT \ln K_{\text{eq}}, \quad (5)$$

from which the mole fraction of *B* can be shown to be

$$X_B = \{1 + \exp[\Delta H - T\Delta S]/RT\}^{-1}, \quad (6)$$

and the associated heat capacity is

$$C_p = (\partial H/\partial T)_p = R(\Delta H/RT)^2 \cdot X_B(1 - X_B). \quad (7)$$

This extra heat capacity is of the Schottky anomaly form,³⁴ a dome with onset commencing at a temperature determined by the molar enthalpy increment per bond break, ΔH , and rapidity of increase and maximum value determined by the associated entropy change, ΔS . The general behavior for different ΔH , ΔS combinations may be seen in Figs. 2 and 3 of Ref. 3, and that for the particular combination $\Delta H = 10.5$ kJ/mol and $\Delta S = 19$ J/mol K is shown at the top of Fig. 7. The dashed line in Fig. 7 shows the heat capacity that remains after the bond-breaking component has been subtracted from the total heat capacity, and it is notable that its relation to the crystal heat capacity is that of a normal glass-former. Thus the anomalous form of the cresol heat capacity is well accounted for. It is notable that the bond energy, 10.5 kJ/mole is that frequently associated with hydrogen bond breaking in hydrogen bonded liquids such as water³⁵ and glycerol.³¹

Cases in which the heat capacity due to a quite separate degree of freedom involving two state excitations is added to an ergodiclike liquid state background well above T_g , have been observed previously³⁶ for the case of a perhalogenated ethane (CFCl_2)₂ (which is actually a plastic crystal). A *cis-trans* isomerism is involved. In this case there is essentially no change of entropy on excitation and the extra C_p contribution can be quantitatively accounted for³⁶ by a simple Schottky expression.³⁴ In that case, the contribution due to the two-state equilibrium froze before the normal T_g for the system was reached, giving rise to an interesting (but very weak) subsidiary glass transition with unusual annealing characteristics.³⁶ The crystallization of mCS in the temperature range where such an ergodicity breaking could occur in the present case, excludes any conclusions about its existence but such an interesting phenomenon, with its multiple liquid state time scale implications, might be observable in mCS-*o*CS mixtures (which would have greater supercooling propensity, see Fig. 3). Such a study will be the subject of future work.

It is to be expected that in cases with hydrogen bonds which are weaker than in cresol (hence less differentiated from the background configurational excitations) the bond-

breaking component will blend with the background and simply increase its magnitude. Indeed this seems a very reasonable way of accounting for the higher (Table II) ΔC_p values, relative to xylene, of fluoroaniline and toluidene—which have weaker $-\text{NH}_2$ -to- NH_2 H-bonds. It will be interesting to see if these differences in thermodynamic properties near T_g will be mirrored by the relaxation behavior in the same temperature regime. At this time there are limited viscosity data near the melting point available in most cases and more extended dielectric relaxation data in selected cases. These will be discussed briefly below.

It is desirable to relate the values of ΔC_p found in this study to values for other molecular liquids, but to do this we must find a way to compensate for the different numbers of atomic groups which can contribute to the configurational freedom of the molecule as a whole. Obviously, complicated molecules like o-terphenyl will have a larger ΔC_p per mole than, for instance, the elemental glassformer selenium. Although often ambiguous, one of the most widely used normalization schemes involves the reduction of the observed ΔC_p value by the number of atoms or groups in a molecule which can, by rotation or reorientation, change the configurational state of a system of such molecules. Such groups were referred to as “beads” by various authors, starting with Wunderlich³⁷ who observed that, for a large number of polymers and molecular liquids, ΔC_p per mole of beads was approximately constant at $11.2 \text{ J mole}^{-1} \text{ deg}^{-1}$. For elemental glasses like computer simulated argon³⁸ Lennard-Jones mixtures³⁹ and selenium,⁴⁰ or ionic glasses like AgCl-CsI^{41} the value is larger, 14–18 J/mole/K. The ambiguity arises when comparing with molecules like 2-methyl hexane, methyl cyclohexane, and toluene, in which the same number of carbon atoms are bound together in different ways, and ways which allow progressively less and less flexibility. Ignoring this problem and treating every carbon, $-\text{F}$, $-\text{NH}_2$, or $-\text{OH}$ as a bead, then there are eight beads per molecule in each member of our series, and the molar value $\Delta C_p/\text{bead}$ ranges from 10.2 (for mTD) down to 6.8 J/mole beads/K (for m-CS), confirming the unusually small value of ΔC_p for the latter case.

An alternative way of comparing heat capacity increases at T_g is to judge them against the heat capacity of their parent crystalline phases. Since atoms strongly bound together (and accordingly not configurationally independent) will usually not reach full vibrational excitation at T_g , this basis of comparison tends to compensate for the above-noted problem of properly defining beads. It is this comparison $\Delta C_p(\text{reduced}) = C_{p,r} = C_p(\text{liquid})/C_p(\text{crystal})$ at T_g , which has been used in some of our previous work^{15,42} The $\Delta C_{p,r}$ values for the present liquids are all quite large, and lead to the expectation of high fragility for the liquid states (see below) The glasses of mFT and mFA, in particular, more than double their heat capacities as the liquidlike degrees of freedom are accessed. Figure 6 shows that, apart from the cases of hydroxyl-containing molecules mCS and mFP, the forms of $C_{p,r}$ vs T are consistent with the hyperbolic temperature dependence required to obtain Eq. (3) from Eq. (1).

D. Kauzmann temperatures, and T_g/T_K in relation to fragility

The relatively large heat capacity changes at T_g discussed in the previous section imply that the liquid excess entropy is being rapidly lost as T_g is approached, and therefore imply, for the present series of liquids, the type of behavior seen in Fig. 2, curve 3. Indeed the Kauzmann temperatures assessed from the usual construction^{3,17} (or from algebraic assessment assuming $\Delta C_p = a + bT$, or alternatively $\Delta C_p = K/T$, for the cases in which the ΔC_p is monotonic) lie, on average, at $0.8T_g$. A particularly simple means of obtaining the Kauzmann temperature is afforded when the hyperbolic temperature dependence of ΔC_p applies. It requires only the value of ΔC_p at T_g [taken as $C_p(\text{liq}) - C_p(\text{cryst})$] and the entropy of fusion ΔS_f for the assessment. By integration of Eq. (2) one obtains

$$S_c(T) = K/T_K - K/T, \quad (8)$$

from which T_K may be obtained as the intercept of the plot of S_c vs $1/T$, in which the position of the line is fixed by ΔS_f and the slope K is $\Delta C_p T_g$. Algebraically, T_K may be obtained from the expression

$$T_K = [\Delta S_f / \Delta C_p T_g + T_m^{-1}]^{-1}. \quad (9)$$

Values of T_K for mFT, mXL, and mTD, obtained using Eq. (9) and data from Tables I and II, have been entered in Table II in parentheses, for comparison with the values obtained by graphical extrapolations incorporating all the C_p data. The agreement is seen to be rather good. As expected from the small change of C_p at T_g due to the absence of the H-bond contribution, which is present at fusion and contributes to ΔS_f , the values of T_K for mFP and mCS estimated using Eq. (9) disagree with graphical estimates (which use all data). The difference is in the required direction [T_K (Eq. (9)) $< T_K$ (graphical)].

While the limitations of DSC precision, and the complexity of some heat capacity functions (mCS and mFP), make the values of T_K obtained in this work less reliable than many others, the average value is meaningful and is rather closer to T_g than the average of previously available data, as assessed in a recent overview.¹⁸ Furthermore, the T_K/T_m value for mTD, 0.61, is almost as high as the most striking case (lactic acid) in Kauzmann's original Fig. 2 type presentation of the entropy paradox. The value for mFA, if it could be crystallized, would doubtless be higher. It is, therefore, of interest to assess their fragilities according to the reduced relaxation time vs reduced temperature relation discussed in connection to Fig. 1. Fortunately a variety of relaxation time data are now available for the liquids in this series,²⁰ and there are also some viscosity data of limited range from standard data sources (e.g., Landolt-Bornstein tables).

To make a scaled temperature comparison of the available data, we adopt the calorimetric 10 K/min T_g values of Table I as scaling temperatures. These are assigned the relaxation time, 100 s, on the basis of previous experience. This is a more appropriate choice than the alternative scaling temperature^{13(a)} at which $\log[\eta/\text{poise}] = 13$ (even when the data are available in this range) since it seems likely that for

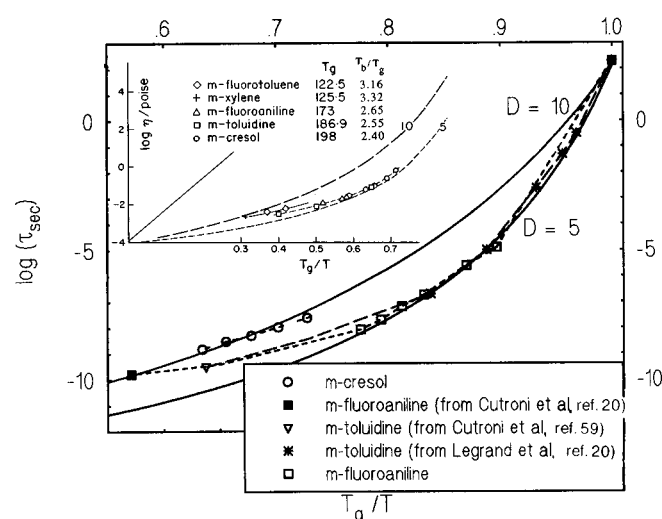


FIG. 8. Dielectric relaxation times for four liquids of this study (Refs. 20,59) plotted in T_g -scaled Arrhenius form, together with curves from Fig. 1 for D values of 5 and 10 to facilitate fragility assessments. Inset: T_g -scaled Arrhenius plots of available viscosity data. Inclusion of data for toluene suggests that lower T_g liquids m-xylene and m-fluorotoluene may be less fragile than the higher T_g , H-bonded, cases. Note the apparently discrepant position of the dielectric data for m-cresol relative to its position for viscosity data.

fragile liquids at temperatures near T_g , the viscous modes can to some extent decouple from the structural relaxation modes.⁴³ It is the latter which carry the thermodynamic strength, and whose relaxation times are expected to diverge as the Kauzmann temperature is approached [Eq. (3)]. The available relaxation time data are plotted vs T_g/T in Fig. 8. Figure 8 includes two plots of Eq. (3) with D values of 5 and 10 for calibration of the present systems. More limited data on the viscosities of five of the liquids, taken from standard data sources, are included in the inset to the figure.

The key observations are twofold. First, with the possible exception of mFT and mXL, these liquids, despite the differences manifested in Fig. 5, appear to be very fragile in character, with D values closer to 5 than 10 (corresponding to steepness indices, m ,⁴⁴ of about 80). Second, m-cresol exhibits dielectric relaxation times that are about one order of magnitude longer than would be expected from its position on the viscosity plot and, in this respect, exhibits an anomalous character seen in some other monoalcohols (most notably n-propanol). The origin of this behavior is incompletely understood, but seems to relate to some sort of H-bond induced clustering of dipoles.

Considering the first observation further, we take the case of mFT for which the relaxation data are most extensive, and for which the ΔC_p data conform at least approximately to the hyperbolic temperature dependence needed to reconcile the VFT equation with the Adam–Gibbs equation, see Eqs. (1)–(3). For such cases, T_o should be the same as T_K , or $T_g/T_o = T_g/T_K$. We can obtain T_g/T_o from D using the relation required⁷ by Eq. (2)

$$T_g/T_o = 1 + D/[2.303 \log(\tau_g/\tau_o)], \quad (10)$$

where $\log \tau_g/\tau_o = 16$ for relaxation times (see Fig. 1). For the

value $D=6$ suggested by the relaxation time findings of Fig. 8, a value of $T_g/T_o = 1.16$ is obtained and this compares favorably with the value, 1.19, from calorimetry given in Table II (1.19 is the value expected for $D=7$). For the cases of m-fluorotoluene and m-xylene, on the other hand, the thermodynamic T_g/T_K values are closer to the value 1.27 expected for $D=10$. Unfortunately only a few viscosity data are available in these cases, but they do in fact fall close to the $D=10$ line (see inset to Fig. 8). Clearly these two cases merit further study.

Of particular interest, though, will be detailed studies of the more complex case of m-cresol where the C_p behavior departs markedly from the hyperbolic form because of the splitting out of the H-bond degrees of freedom. Note that the fragile behavior implied by the viscosity is observed only in the region where the excess C_p is large. It is important to establish the relation between thermodynamic and relaxation properties in such cases—of which we believe a number exist (Sichina and Angell, unpublished work). The complex relaxation behavior of the much-studied^{45–47} OH-containing liquid, salol, may be expected to find its origin in a similar inhomogeneity in the molecular interactions consequent on the presence of OH–OH interactions.

The latter case is also that in which the second notable feature of Fig. 8 arises: This is the apparent separation of time scales in dielectric and shear relaxation. In the previous cases of such time scale separations, H-bonding has also been implicated though the precise mechanism has not been clarified.⁴⁸ Cases such as the present one, in which even thermodynamic properties detect the effects, should help to clarify the general problem. From an inspection of available melting and boiling point data, it seems that m-ethyl phenol may be a better case for study, as crystallization will probably not interfere ($T_b/T_m = 1.83$ vs 1.69 for m-cresol).

V. CRYSTALLIZATION AND THE KAUZMANN PARADOX

The question of what happens between T_g and T_K under semi-infinitely slow cooling remains an open question at this time. Kauzmann originally argued that the nucleation barrier to crystallization would disappear between T_g and entropy crossover temperature, but various authors including one of us^{49,50} have argued, on the assumption that nucleation rates are eventually dominated by the viscosity relaxation time, that in many cases the relaxation to the more stable amorphous state would always be faster than that to the crystal. However, the promotion of crystallization in m-toluidine by cooling to below the β -glass transition temperature is suggestive of an alternative view based on the recent theoretical⁵¹ and experimental^{52,53} evidence that crystal nucleation kinetics depend critically on the “fast” regions of the inhomogeneous structures now being increasingly identified in fragile glassformers near T_g .

The β -glass transition has now²² been convincingly associated with the familiar β -relaxation (now called “slow β ” to distinguish it from the fast process of MCT) and is now being associated with the movement of molecules in the fast regions of the inhomogeneous liquid structure.^{53,54} If this proves to be the case then, in view of the Arrhenius tempera-

ture dependence of the β -relaxation, nucleation (if not significant growth) could still proceed at the Kauzmann temperature and Kauzmann's original argument would be resuscitated. In this case the salvation of the ideal glass concept will depend on a demonstration that the strength of the β -process (which must reflect the number of molecules remaining in fast regions) approaches zero as the glass is annealed below the normal T_g —and vanishes as the Kauzmann temperature is approached. Indeed, this is the interpretation of Perrera and Harrowell⁵⁴ in their inhomogeneous liquid approach to the dynamics of glassforming liquids relaxation dynamics. It is also consistent with the failure, in some cases (such as the fragile propylene carbonate), to find a β -glass transition even with the very high sensitivity of the adiabatic calorimetry experiments of Oguni and colleagues.^{22,55} We hope to investigate this matter further in future work.

VI. CONCLUDING REMARKS

This work has demonstrated how, as the interactions in a molecular liquid are made increasingly heterogeneous, a changeover from homogeneous to multimodal configurational excitation can be promoted. The case of cresol discussed in this paper is, in retrospect, not the only case of such serial configurational excitations due to inhomogeneous interactions to be reported. A related case is that in which van der Waals interactions were excited configurationally at temperatures below those at which Coulomb interactions could be overcome. In this case⁵⁶ two successive glass transitionlike heat capacity steps, implying well separated excitation time scales, could be observed, but the observations were interpreted in terms of a strong secondary relaxation in the *glassy* state preceding the “real” glass transition. There may be a subtle distinction here, between secondary relaxations and serial components of the primary relaxation, which will require further work to elucidate. The existence of a hierarchy of systems with two-state complexity within the liquid state, i.e., above the “ T_g ” which is associated with shear relaxation times of order 100 s, has been suggested⁵⁷ and warrants further study.

ACKNOWLEDGMENTS

This work was supported by the National Science Foundation under Solid State Chemistry Grant Nos. DMR 8304887 (Purdue University) and DMR 9108028-002 (Arizona State University).

¹J. P. Stoessel and P. G. Wolynes, *J. Chem. Phys.* **80**, 4502 (1984); R. W. Hall and P. G. Wolynes, *ibid.* **86**, 2943 (1987).

²C. A. Angell, *J. Am. Chem. Soc.* **51**, 117 (1968); C. A. Angell and K. J. Rao, *J. Chem. Phys.* **57**, 470 (1972).

³U. Buchenau and R. Zorn, *Europhys. Lett.* **18**, 523 (1992); U. Buchenau, *J. Non-Cryst. Solids* **172–174**, 391 (1994); *Philos. Mag.* **65**, 303 (1992).

⁴G. Adam and J. H. Gibbs, *J. Chem. Phys.* **43**, 139 (1980).

⁵M. H. Cohen and D. Turnbull, *J. Chem. Phys.* **31**, 1164 (1959); M. H. Cohen and G. S. Grest, *Adv. Chem. Phys.* **48**, 370 (1981); *Phys. Rev. B* **24**, 4091 (1981).

⁶T. Gesztz, *J. Phys. C* **101A**, 477 (1980); E. Leutheusser, *Phys. Rev. A* **29**, 2765 (1984); U. Bengtzelius, W. Gotze, and A. Sjolander, *J. Phys. (France)* **17**, 5915 (1984); W. Götze in *Liquids, Freezing, and the Glass Transition*, edited by J. P. Hansen and D. Levesque (NATO-ASI, North

Holland, Amsterdam, Les Houches, 1989), 287–503; W. Götze and L. Sjögren, *Rep. Prog. Phys.* **55**, 55 (1992).

⁷U. Bengtzelius and L. Sjögren, *J. Chem. Phys.* **84**, 1744 (1986); H. Sillescu and E. Bartsch, in *Disorder Effects on Relaxational Processes*, edited by R. Richert and A. Blumen (Springer Verlag, 1993), p. 55–88.

⁸D. Kivelson, S. Kivelson, X. Zhao, Z. Nussinov, and G. Tarjus, *Physica B* **27**, (1995).

⁹C. A. Angell, F. H. Stillinger, B. Frick, D. Richter, I. M. Hodge, and L. Greer, *Science* **267**, 5 (1995).

¹⁰J. H. Gibbs and E. A. Dimarzio, *J. Chem. Phys.* **28**, 373 (1958).

¹¹M. Goldstein, *J. Chem. Phys.* **51**, 3728 (1969); F. H. Stillinger and T. A. Weber, *Phys. Rev. A* **25**, 978 (1982); **28**, 2408 (1983); F. H. Stillinger and T. A. Weber, *Science* **225**, 983 (1984).

¹²M. Goldstein, *J. Chem. Phys.* **64**, 4767 (1976).

¹³(a) C. A. Angell, in *Relaxations in Complex Systems*, edited by K. Ngai and G. B. Wright (National Technical Information Service, U.S. Department of Commerce, Springfield, VA 22161 1985), p. 1; (b) C. A. Angell, *J. Phys. Chem. Solids* **49**, 863 (1988).

¹⁴R. Böhmer and C. A. Angell, in *Disorder Effects on Relaxational Processes*, edited by A. Blumen and R. Richert (Springer Verlag, Berlin, 1994), p. 11.

¹⁵C. Alba, L. E. Busse, and C. A. Angell, *J. Chem. Phys.* **92**, 617 (1990).

¹⁶W. Kauzmann, *Chem. Rev.* **43**, 219 (1948); C. A. Angell, *J. Chem. Educ.* **47**, 583 (1970).

¹⁷C. A. Angell, *J. Res. NIST* **102**, 171 (1997).

¹⁸F. H. Stillinger, *J. Chem. Phys.* **88**, 7818 (1988).

¹⁹H. Senapati (unpublished work).

²⁰C. Alba-Simionesco, *J. Chem. Phys.* **100**, 2250 (1994); C. Alba-Simionesco and M. Krauzmann, *ibid.* **102**, 6574 (1995); M. Cutroni, P. Migliardo, A. Piccolo, and C. Alba-Simionesco, *J. Phys.: Condens. Matter* **6**, 5283 (1994); V. Legrand *et al.*, *Thermochimica Acta* (in press); H. Fujimori *et al.*, *Prog. Theor. Phys.* **126**, 229 and 235, (1997).

²¹O. Yamamuro, I. Tsukushi, A. Lindqvist, S. Takahara, M. Ishikawa, and T. Matsuo, *J. Phys. Chem. B* **102**, 1605 (1998).

²²H. Fujimori and M. Oguni, *Solid State Commun.* **94**, 157 (1995).

²³Q. Lu, V. Velikov, and C. A. Angell (to be published).

²⁴S. Seki and H. Suga, *J. Non-Cryst. Solids* **16**, 171 (1974).

²⁵D. Turnbull and M. H. Cohen, *J. Chem. Phys.* **29**, 1049 (1958).

²⁶C. A. Angell, A. Dworkin, P. Figuiere, A. Fuchs, and H. Szwarc, *J. Chim. Phys.* **82**, 773 (1985).

²⁷S. Sakka, K. Matsuita, and K. Kamiya, *Phys. Chem. Glasses* **20**, 25 (1979); S. Sakka, *Annu. Rev. Mater. Sci.* **16**, 29 (1986).

²⁸J. L. Green and C. A. Angell (unpublished work).

²⁹W. A. P. Luck and W. Ditter, *J. Phys. Chem.* **74**, 482 (1969).

³⁰C. A. Angell and D. L. Fields, *J. Phys. Chem.* **89**, 4565 (1985).

³¹A. Barkatt and C. A. Angell, *J. Chem. Phys.* **70**, 901 (1979).

³²C. Bois, *Acta Crystallogr., Sect. B: Struct. Crystallogr. Cryst. Chem.* **29**, 1011 (1973).

³³C. A. Angell, *J. Phys. Chem.* **75**, 3698 (1971).

³⁴C. Kittel, *Introduction to Solid State Physics*, 2nd ed. (Wiley, New York, 1956).

³⁵G. E. Walrafen, *J. Chem. Phys.* **52**, 4176 (1970); G. E. Walrafen, *Water, a Comprehensive Treatise*, edited by F. Franks (Plenum, New York, 1971), Chap. 6.

³⁶K. Kishimoto, H. Suga, and S. Seki, *Bull. Chem. Soc. Jpn.* **51**, 1691 (1978).

³⁷B. Wunderlich, *J. Phys. Chem.* **64**, 1052 (1960).

³⁸J. H. R. Clarke, *J. Chem. Soc., Faraday Trans. 2* **76**, 1667 (1976).

³⁹K. Vollmayr, W. Kob, and K. Binder, *Phys. Rev. B* **54**, 15808 (1996).

⁴⁰S. S. Chang and A. B. Bestul, *J. Chem. Thermodyn.* **6**, 325 (1974).

⁴¹L. M. Torell, D. C. Ziegler, and C. A. Angell, *J. Chem. Phys.* **81**, 5053 (1984).

⁴²C. A. Angell and W. Sichina, *Ann. (N.Y.) Acad. Sci.* **279**, 53 (1976).

⁴³C. A. Angell, *J. Non-Cryst. Solids* **102**, 205 (1988); Shear relaxation becoming faster than structure equilibration near T_g would be consistent with the development near T_g of microheterogeneities in the structure, for which evidence is accumulating [M. T. Cicerone and M. D. Ediger, *J. Chem. Phys.* **103**, 5684 (1995); M. T. Cicerone, F. R. Blackburn, and M. D. Ediger, *ibid.* **102**, 471 (1995)]. However, the low values of shear viscosity η_s observed at T_g could also be rationalized if fragile liquids have particularly low high frequency shear moduli G_∞ , since the Maxwell relation $\eta_s = G_\infty \tau_s$ would then permit τ_s to remain at the structural relaxation value [S. R. Nagel, in *Phase Transitions and Relaxation in Systems*

- with *Competing Energy Scales*, edited by T. Riste and D. Sherrington (Kluwer Academic, Netherlands, 1993), p. 259].
- ⁴⁴D. J. Plazek and K. L. Ngai, *Macromolecules* **24**, 1222 (1991).
- ⁴⁵P. K. Dixon, *Phys. Rev. B* **42**, 8179 (1990); W. T. Laughlin and D. R. Uhlmann, *J. Phys. Chem.* **76**, 2317 (1972).
- ⁴⁶F. Stickel and E. M. Fischer, *Physica A* **201**, 263 (1993); M. E. Carpenter, D. B. Davies, and A. J. Matheson, *J. Chem. Phys.* **46**, 2451 (1967).
- ⁴⁷R. Richert and C. A. Angell, *J. Chem. Phys.* **108**, 9016 (1998).
- ⁴⁸C. Hansen and R. Richert, *J. Chem. Phys.* **107**, 1 (1996).
- ⁴⁹C. A. Angell, D. R. MacFarlane, and M. Oguni, *Ann. (N.Y.) Acad. Sci.* **484**, 286 (1986).
- ⁵⁰D. J. J. Zelinski, H. Yinnon, and D. R. Uhlmann, *Glastech. Ber.* **56K**, 822 (1983).
- ⁵¹P. Harrowell and D. W. Oxtoby, *Ceram. Trans.* **30**, 35 (1993).
- ⁵²N. Okamoto and M. Oguni, *Solid State Commun.* **99**, 53 (1996).
- ⁵³T. Hikima, M. Hanaya, and M. Oguni, *Bull. Chem. Soc. Jpn.* **69**, 1863 (1996).
- ⁵⁴D. Perrera and P. Harrowell, *Phys. Rev. E* **54**, 1652 (1996).
- ⁵⁵M. Oguni, (private communication).
- ⁵⁶J. Fan and C. A. Angell, *J. Phys. Chem.* **98**, 9345 (1994).
- ⁵⁷C. A. Angell, *Prog. Theor. Phys.* **126**, 1 (1977).
- ⁵⁸R. J. L. Andon, J. F. Counsell, E. B. Lees, J. F. Martin, and C. J. Marsh, *Trans. Faraday Soc.* **63**, 1115 (1967).
- ⁵⁹M. Cutroni, P. Migliardo, A. Piccolo, and C. Alba-Simionesco, *J. Phys.: Condens. Matter* **6**, 5283 (1994).
- ⁶⁰J. Phys. Chem. Ref. Data **13**, 148 (1984).